Research highlight

Maryam Eskandari-Nojehdehi, Hoda Jafarizadeh-Malmiri* and Javad Rahbar-Shahrouzi

Optimization of processing parameters in green synthesis of gold nanoparticles using microwave and edible mushroom (*Agaricus bisporus*) extract and evaluation of their antibacterial activity

DOI 10.1515/ntrev-2016-0064
Received August 3, 2016; accepted August 9, 2016; previously published online September 17, 2016

Abstract: Gold nanoparticles (AuNPs) were synthesized using edible mushroom *Agaricus bisporus* extract as both reducing and stabilizing agents via microwave irradiation method. The effects of the microwave exposure time and the amount of $HAuCl_4$ solution (1 mM) on the mean particle size, concentration, and polydispersity index (PDI) of the synthesized AuNP solution were investigated using response surface methodology. Mushroom extract was characterized by Fourier transform infrared. The synthesized AuNPs were characterized by dynamic light scattering, UV-Vis spectroscopy, and transmission electron microscopy. Well-dispersed and spherical AuNPs with the minimum mean particle size and PDI, and maximum concentration and zeta potential of 33.56 ± 1.8 nm, 0.855 ± 0.02 ppm, 148.88 ± 2.7 ppm, and +17.2 mV, respectively, were obtained using 2.62 ml of $HAuCl_4$ and 0.2 ml of mushroom extract for 55 s. The antibacterial activity of the fabricated AuNPs was assessed against both Gram-negative (*Escherichia coli*) and Gram-positive (*Staphylococcus aureus*) bacteria and was found to be possessing high bactericidal effects.

Keywords: antibacterial activity; green synthesis; gold nanoparticles; microwave irradiation; mushroom extract.

***Corresponding author: Hoda Jafarizadeh-Malmiri,** Faculty of Chemical Engineering, Sahand University of Technology, Tabriz 1996-51335, Iran, e-mail: h_jafarizadeh@sut.ac.ir; h_jafarizadeh@yahoo.com
Maryam Eskandari-Nojehdehi and Javad Rahbar-Shahrouzi: Faculty of Chemical Engineering, Sahand University of Technology, Tabriz 1996-51335, Iran

1 Introduction

Gold nanoparticles (AuNPs) have gained much more attention because of their biocompatibility, noncytotoxicity, and fascinating properties such as facile synthesis and surface modification. These unique properties make them much usable in the fields of biotechnology and biomedicine. In fact, AuNPs have considerable potential applications in nanomedicine, new category catalysis medicine, nano-optoelectronics, and drug delivery [1, 2]. Furthermore, AuNPs also pose bactericidal and fungicidal activity against many different microorganisms [3, 4]. AuNPs can be produced using the top-down (physical) and the bottom-up (chemical and biological) methodologies [5]. The chemical synthesis methods are simple and easy control. However, they generate toxicity because of unwanted harmful interactions with biological systems [6, 7]. Numerous physical methods (i.e. sonochemical, ultrasound irradiation, ultraviolet [UV] irradiation, and hydrothermal) have been applied to synthesis nanoparticles (NPs). However, these techniques are expensive and unsustainable [7–10]. The microwave irradiation represents a relatively new strategy in NP synthesis [11]. Microwave heating has numerous advantages over the conventional heating methods such as achieving high temperatures within a limited time (under a pressure controlled environment), greater control on heating rates, and uniform heat distribution [12, 13]. Furthermore, moving of the metal NPs is accelerated in the microwave electric field because they carry electrical charges. Therefore, the growth of particles by coagulation is decreased in microwave plasma [11]. Several studies have been conducted to synthesize uniform and more stable metal NPs using microwave [11, 13, 14]. However, a few studies have synthesized AuNPs using microwave heating [15, 16].

Recently, AuNP synthesis by using plant extracts and microorganisms has gained much attention as an

alternative approach [17, 18]. Edible mushrooms have received much attention in NP synthesis because of their numerous reducing biomolecules such as flavonoids, phenolic acids, tannins, and oxidized polyphenols [19, 20]. Furthermore, mushroom extract contains high protein content, and the carbonyl group of its amino acids has a high capability to prevent the agglomeration of the NPs and, consequently, stabilize them in aqueous solution [5]. Few studies have been conducted on the production of AuNPs using different edible mushroom extracts such as *Pleurotus florida* and *Volvariella volvacea* [20, 21].

Up to now, there is no comprehensive study on AuNP synthesis using edible mushroom extract under microwave irradiation. Therefore, the main objectives of the present study were (i) to evaluate the potential of mushroom extract as a green reducer and stabilizer for AuNP synthesis, (ii) to optimize the synthesis conditions to fabricate stabilized AuNPs with smaller particle size and PDI and high concentration, and (iii) to investigate the final antibacterial activity of the synthesized AuNPs.

2 Materials and methods

2.1 Materials

Fresh mushroom *Agaricus bisporus* (white button mushroom) was provided from local market in Tabriz, Iran. Gold salt (HAuCl4) was purchased from Sigma-Aldrich (Sigma-Aldrich Co., St. Louis, MO). The standard solution of AuNPs (with particle size of 10 nm and concentration of 100 ppm) was obtained from Tecnan-Nanomat (Navarra, Spain). To prepare all aqueous solutions, deionized double-distilled water was used.

Escherichia coli (PTCC 1270) and *Staphylococcus aureus* (PTCC 1112) were purchased from microbial Persian type culture collection (PTCC, Tehran, Iran). Nutrient agar (NA) and nutrient broth (NB) were purchased from Biolife (Biolife Co., Milan, Italy).

2.2 Preparation of aqueous mushroom extract

The mushrooms were washed thoroughly three times with distilled water to remove the impurities and then shade dried for 3 days and powdered using domestic miller (MX-GX1521; Panasonic, Tokyo, Japan). Five grams of the mushroom powder was added into 100 ml of distilled water and boiled for 10 min. After that, it was filtered through Whatman No. 1 filter paper, and the resulting mushroom extract was collected and kept in the refrigerator at 4°C.

2.3 AuNP synthesis using mushroom extract

The AuNP solution was obtained by a domestic microwave-assisted synthetic approach. $HAuCl_4$ solution (1 mM) was provided by dissolving 0.392 g of its powder in 100 ml of deionized double-distilled water. In a typical synthesis, different amounts of $HAuCl_4$ (1–11 ml) was mixed with 0.2 ml of mushroom extract, and then the mixture solution was heated using microwave oven (MG-2312W, LG Co., South Korea) at constant power of 800 W at different microwave exposure times (30–60 s).

2.4 Physicochemical assay

2.4.1 Fourier transform-infrared (FT-IR) spectra analysis

To identify the possible reducing and stabilizing biomolecules of mushroom extract, Fourier transform-infrared (FT-IR) measurements were conducted. The FT-IR spectra of mushroom extract were recorded on a Bruker Tensor 27 spectrometer (Bruker, Germany) using KBr pellets in the 4000–400-cm^{-1} region [22].

2.4.2 pH determination

Generally, NP formation is greatly affected by the pH value of the plant extract. The pH level of the prepared mushroom extracts was measured using a pH meter (DELTA 320, Shanghai, China).

2.4.3 Surface plasmon resonance

AuNP synthesis was investigated by scanning the reacting mixture under a spectrophotometer because of their surface plasmon resonance (SPR), which can induce a strong absorption of the incident light. Therefore, the absorption spectrum of the solutions were taken with a UV-Vis spectrophotometer using a Jenway UV-Vis spectrophotometer 6705 (UK) in a 1-cm optical path quartz cuvette. It can be observed that broad emission peaks (λ_{max}) were centered (510–570 nm) because of the presence of surface plasmon vibration bands, which in turn can change the color of the mixture solution to a striking ruby red in various media [15]. The intensity and wavelength of the SPR band of NPs can

be related to some factors such as the metal type, shape, and size of the NPs, dielectric constant, and composition of the mixture solution, which may influence the density of the electron charge on the surface of NPs [1].

2.4.4 Concentration of the AuNP synthesis

UV-Vis spectroscopy measurements may also be used to estimate the concentration of AuNPs in the solution. In fact, the concentration of formed AuNPs is proportional to the absorbance of the AuNP solution. To measure the concentration of synthesized AuNPs, the standard curve has been established using several serial dilute solutions of AuNPs (10–100 ppm) from a standard solution of AuNPs (100 ppm). The concentration of the sample was achieved by comparison of the absorbance of the synthesized NPs with the standard curve.

2.4.5 Particle size and particle size distribution

A dynamic light scattering (DLS) particle size analyzer (Nanotrac Wave, Microtrac, USA) was used to assess the mean particle size, the particle size distribution (PSD), and the polydispersity index (PDI) of the produced AuNPs at 25°C. DLS technique scatters a laser light beam at the surface of dispersed NPs, which results in the detection of the backscattered light. PDI is a dimensionless value that shows the uniformity of the synthesized NPs. Fine and narrow PSD can be obtained when it shifts toward 0 [23].

2.4.6 Zeta potential

The zeta potential (surface charge) measurement is an approximation value related to the NPs surface electric charge, which is an indirect description of the physical stability of the synthesized NPs in the mixture solution. The zeta potential of green synthesized AuNPs was determined at 25°C using DLS (Nanotrac Wave, Microtrac, USA). Water was used as dispersant, and measurements were conducted in triplicates.

2.4.7 Transmission electron microscopy

Transmission electron microscopy (TEM) was used to evaluate of the synthesized AuNPs morphology. A drop of formed AuNP solution was placed on a carbon-coated copper grid, and its morphological assay was conducted using a TEM (CM120, Philips, Amsterdam, Netherlands) with an acceleration voltage of 120 kV.

2.5 Antibacterial assay

For the evaluation of the antibacterial activity of synthesized AuNPs, the effect of NPs was tested on the provided bacterial suspensions. In fact, the bacterial species were inoculated on an NA media plate for 18–24 h at 37°C. Three to five well-isolated colonies of the same morphological type were mixed in 10–15 ml of sterile normal saline solution. Bacterial suspension density was adjusted to 0.5 McFarland standard, which has an absorbance of 0.08–0.10 at 625 nm. This is equivalent to 1.5×10^8 colony-forming units of bacteria in 1 ml of prepared inoculums [24].

In a 96-well plate, 130 µl of double-strength NB, 10 µl of AuNPs, and 10 µl of prepared bacterial suspensions were mixed. Positive control wells contained 140 µl of NB and 10 µl of standard inoculum, whereas negative control wells contained 150 µl of NB. The provided 96-well plate was then shaken for 15 s, and the absorbance (turbidity) of the wells was measured using a microplate reader (DA-3200; DANA, Tehran, Iran) at 26.1°C. After that, the provided 96-well plate was incubated at 37°C for 24 h, and the absorbance (turbidity) of the wells was measured again. The antibacterial activity of synthesized AuNPs was judged by the lack of turbidity in the wells. In other words, during the incubation of the 96-well plate, the bacteria grew in the wells and increased their population, which in turn increased the turbidity of the well media. However, the presence of AgNPs in the well media inhibited the growth of bacteria because of their antibacterial activity, and the turbidity of the well media did not change after the incubation of the plate.

2.6 Experimental design and statistical analysis

The experiment was planned using a central composite design, and response surface methodology (RSM) was used to evaluate the effects of two independent parameters, namely, microwave exposure time (X_1) and amount of $HAuCl_4$ solution (X_2), on the prepared AuNPs. The studied response variables were concentration (Y_1, ppm), mean particle size (Y_2, nm), and PDI (Y_3) of the synthesized AuNPs. As clearly observed in Table 1, 13 experimental treatments were assigned with five different levels for each independent parameter using the Minitab software (v.16 statistical package; Minitab Inc., State College, PA). In the randomized experimental runs, the center point ($X_1 = 45$ min and $X_2 = 6$ ml) was repeated five times to minimize pure error. RSM has numerous advantages, making it highlighted as compared with the classic one-variable-at-a-time optimization. For example, it generates numerous valuable data using a few experimental runs to obtain

Table 1: Experimental runs according to the central composite design and response variables for AuNP synthesis.

Sample number	Microwave exposure time (s)	Amount of $HAuCl_4$ (ml)	Particle size (nm)		Concentration (ppm)		PDI	
			Exp	Pre	Exp	Pre	Exp	Pre
1	45.0	6.00	42.3	41.0	149.47	151.21	1.22	1.23
2	34.4	2.46	38.3	36.7	132.02	135.12	0.89	1.01
3	55.6	2.46	31.6	33.1	150.00	146.90	0.78	0.87
4	45	6.00	41.6	41.0	152.45	151.21	1.22	1.23
5	45	6.00	39.2	41.0	151.70	151.21	1.60	1.30
6	34.4	9.53	20.0	18.5	83.09	86.19	0.82	0.86
7	55.6	9.53	65.6	67.2	144.68	141.58	1.11	0.80
8	45.0	11.00	48.6	44.77	151.70	151.21	0.56	0.71
9	45.0	1.00	47.6	38.7	149.57	151.21	0.89	0.76
10	45.0	6.00	41.0	41.0	151.21	151.20	1.23	1.23
11	45.0	6.00	41.0	41.0	151.21	151.20	1.23	1.23
12	30.0	6.00	37.0	39.2	97.13	92.74	1.48	1.39
13	60.0	6.00	73.3	71.1	135.85	140.23	0.51	0.47

Exp, experimental values of studied responses; Pre, predicted values of studied responses.

suitable models, which can predict responses in the defined independent variable ranges. Furthermore, RSM is a feasible method to estimate the interactions of independent variables on the responses. Therefore, it is a proper technique that can be used to optimize the main independent parameters of the process [25, 26]. To correlate the mean particle size (Y_1), concentration (Y_2), and PDI (Y_3) of the synthesized AuNPs to the studied synthesis variables, a second-order polynomial equation (Equation 1) was used:

$$Y = \beta_0 + \beta_1 X_1 + \beta_2 X_2 + \beta_{11} X_1^2 + \beta_{22} X_2^2 + \beta_{12} X_1 X_2, \quad (1)$$

where β_0 is a constant, and β_i, β_{ii}, and β_{ij} correspond to the linear, quadratic, and interaction effects, respectively. The suitability of the model was studied accounting for the coefficient of determination (R^2) and adjusted coefficient of determination (R^2-adj). Analysis of variance was also used to provide the significant determinations of the resulted models in terms of p value and F ratio. High values of F ratio and small p values (lower than 0.05) were considered as statistically significant. On the basis of the fitted polynomial equations, three-dimensional surface plots and two-dimensional contour plots were designed to visualize the independent variable interactions [27]. It should be considered that the responses can be predicted thoroughly using the obtained models within the defined ranges for the independent variables.

2.7 Optimization and validation procedure

To obtain the optimum values for microwave exposure time and the amount of $HAuCl_4$ solution with the desired response variables, numerical multiple response and graphical optimizations were used [25]. In fact, optimal conditions for the independent parameters were obtained by estimating the resulted surface plots with limitations on the responses of a minimum value for mean particle size and PDI as well as a maximum value of AuNP concentration. Finally, for verification of the validity of the statistical experimental approaches, three additional approval tests were performed at obtained optimum synthesis conditions.

3 Results and discussion

3.1 Mushroom extract specifications

The FT-IR spectrum of mushroom extract is shown in Figure 1. As clearly observed in the spectrum, several absorption peaks were centered at 1150.07, 1450.23, 1637.84, 2066.60, and 3476.69 cm^{-1}. The absorption peak centered at 1150.07 cm^{-1} referred to the C-O stretch vibration, which could be related to the Ester linkages. The wave number of 1450.23 cm^{-1} was corresponded to the carbonyl, NH, and NH_2. The intense peak at 1637.84 cm^{-1} was related to amide I, which was created because of the vibrations of carbonyl stretch bonded to the protein. It seems that the proteins have binding ability with Au ions, which in turn creates a surrounded layer on the AuNPs and acts as a capping agent to decrease AuNP agglomeration and increases their stability in the medium [21]. The peak at 2066.60 cm^{-1} corresponded to the C=N bond, and the most wide spectrum absorption peak was observed at 3476.69 cm^{-1}. It can be

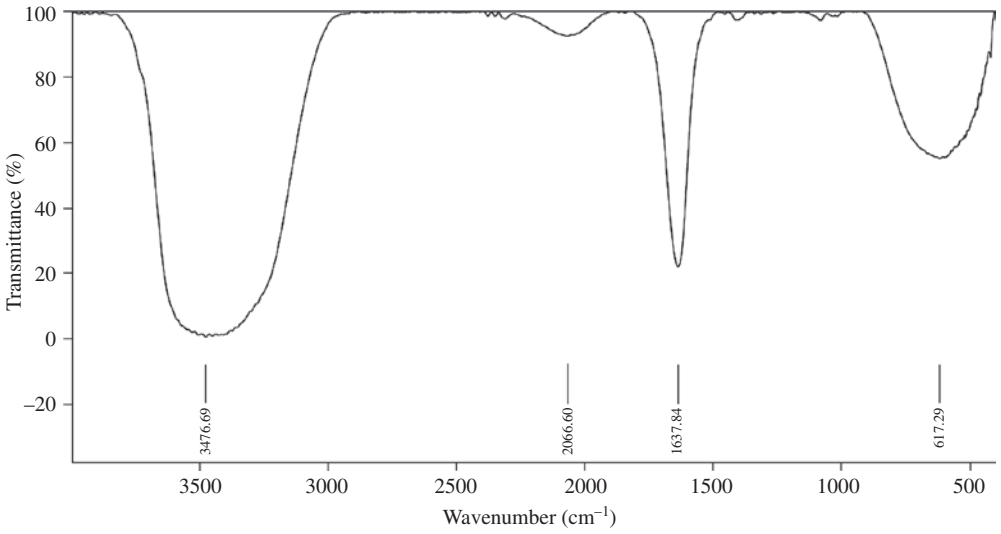

Figure 1: FT-IR spectrum of mushroom extract.

referred to the stretching vibration of primary amines and hydroxyl groups (–OH), which were related to the proteins, and flavonoids, phenolic acids, tannins, and carbohydrate of the mushroom extract were responsible for reducing the Au ions to atoms [20]. The obtained results were in agreement with the finding of Narasimha et al. [28]. They indicated that the main compounds and functional chemical groups of *A. bisporus* were proteins, carbohydrates, dietary fibers, carbonyl groups, hydroxyl, and carboxylic acids, which acted as reducing and stabilizing agents in the silver NP synthesis. The mean pH of the prepared mushroom extract was approximately 6.02, indicating that the mushroom extract is an acidic solution.

3.2 Fitting the response surface models

According to the achieved values for the designed experiments (Table 1) and by applying multiple regression analysis, second-order polynomial models for studying two AuNP synthesis parameters were fitted. The estimated regression coefficients and the corresponding significance of regressions for the models are given in Table 2.

F ratio and p values of all the main, quadratic, and interaction terms of the obtained final models are also shown in Table 3. Generally, higher *F* ratio and lower p value indicate higher importance of the chosen term on the responses.

High values of the R^2 and R^2-adj for the obtained models were a good measure for the overall performance of the models and their accuracy. Moreover, the obtained insignificant lack of fits for achieved models confirmed their sufficient fitness to the synthesis parameter effects

Table 2: Regression coefficients, R^2, R^2-adj, and probability values for the fitted models.

Regression coefficient	Particle size (nm)	PDI	Concentration (ppm)
β_0 (constant)	181.145	–2.643	–149.39
β_1 (main effect)	–6.675	0.127	13.73
β_2 (main effect)	–5.729	0.660	–10.78
β_{11} (quadratic effect)	0.063	–0.001	–0.154
β_{22} (quadratic effect)	–0.737	–0.037	–0.512
β_{12} (interaction effect)	0.349	–0.006	0.291
R^2	98.86%	93.38%	98%
R^2-adj	97.72%	85.11%	97.16%
Lack of fit	14.67	4258.67	64.04
p-Value (regression)	0.019	0.000	0.001

β_0 is a constant, and β_i, β_{ii}, and β_{ij} are the linear, quadratic, and interaction coefficients of the quadratic polynomial equation, respectively.
1, microwave exposure time (s); 2, amount of $HAuCl_4$ (ml).

Table 3: p-Value and *F* ratio of the regression coefficients in the obtained models.

Main effects	Main effects		Quadratic effects		Interacted effects
	X_1	X_2	X_{11}	X_{22}	X_1X_2
Particle size (Y_1, nm)					
p-Value	0.000	0.032	0.001	0.001	0.000
F ratio	75.52	8.62	57.68	40.45	138.43
Concentration (Y_2, ppm)					
p-Value	0.000	0.029	0.000	0.060	0.003
F ratio	96.40	9.20	105.30	5.90	29.09
PDI (Y_3)					
p-Value	0.033	0.014	0.034	0.006	0.057
F ratio	10.13	17.47	10.00	28.74	7.03

1, microwave exposure time (s); 2, amount of $HAuCl_4$ (ml).

(Table 2). As clearly observed in Table 3, the main terms of the synthesis variables had significant ($p < 0.05$) effects on all responses of the synthesized AuNPs. The obtained results indicated that the main term of microwave exposure time (X_1) had the most significant ($p < 0.05$) effect on AuNP concentration and mean particle size of the formed AuNPs because of their small p values. However, the amount of $HAuCl_4$ solution (X_2) was the most effective parameter on the PDI of the produced AuNPs. The results also indicated that the quadratic term of the microwave exposure time had a significant effect ($p < 0.05$) on all studied responses. However, the amount of $HAuCl_4$ solution had an insignificant effect on the synthesized AuNP concentration. The results also revealed that the interaction effect of independent parameters had an insignificant effect on the PDI of the synthesized AuNPs.

3.3 Particle size of synthesized AuNPs

The mean particle size of the synthesized AuNPs ranged from 20.0 to 73.3 nm (Table 1). The obtained results indicated that AuNPs could be synthesized using natural reductants existing in mushroom extract without applying other chemical-reducing agents. The AuNP size changes could also be explained as a function of microwave exposure time and the amount of $HAuCl_4$ solution (Figure 2). The resulted regression coefficients and their p values and *F* ratios revealed that the main effects of both independent variables had a negative effect on the mean particle size of the synthesized AuNPs. However, the quadratic terms of the amount of $HAuCl_4$ solution and microwave exposure time affected the particle size, negatively and positively, respectively (Table 2). It means that increasing either microwave exposure time or amount of $HAuCl_4$ solution at their lower levels, and also the amount of $HAuCl_4$ at high levels, led to a small decrease in the mean particle size of the formed NPs. However, at high levels, the mean particle size of the created AuNPs was increased considerably by increasing the microwave exposure time. The interaction effect of synthesis parameters was also found to be significant ($p < 0.05$) on the mean particle size of AuNPs (Table 3). As clearly observed in Figure 2A, at either low or high amounts of $HAuCl_4$, by increasing the microwave exposure time, the particle size of the formed AuNPs decreased and increased, respectively. In fact, minimum particle size was obtained at minimum microwave exposure time and maximum amount of $HAuCl_4$ solution, and maximum particle size was formed at maximum microwave exposure time and $HAuCl_4$ amount (Figure 2B). The obtained result can be explained by the fact that at high amounts of $HAuCl_4$ solution, by increasing the microwave exposure time, the temperature of the colloidal solution increased. The higher kinetic energy of the Au ions at higher temperature increased their collision rate, which in turn increased the opportunities of the nucleation and growth of the NPs [29]. Therefore, the particle size of AuNP synthesis was decreased by increasing the microwave exposure time during the synthesis procedure. The obtained results were in agreement with the finding of Zhang et al. [29]. They found that the particle size of AuNP synthesis with aqueous aloe vera leaf extract was increased with the increasing of temperature of synthesis procedure. However, it seems that at low amounts of $HAuCl_4$, the carbonyl group of proteins (band at 1637.84 cm^{-1} in Figure 1) formed a covering layer around the metal ions that prevented their agglomeration and enhanced the stability of the solution. Medda et al. [30] found similar results during

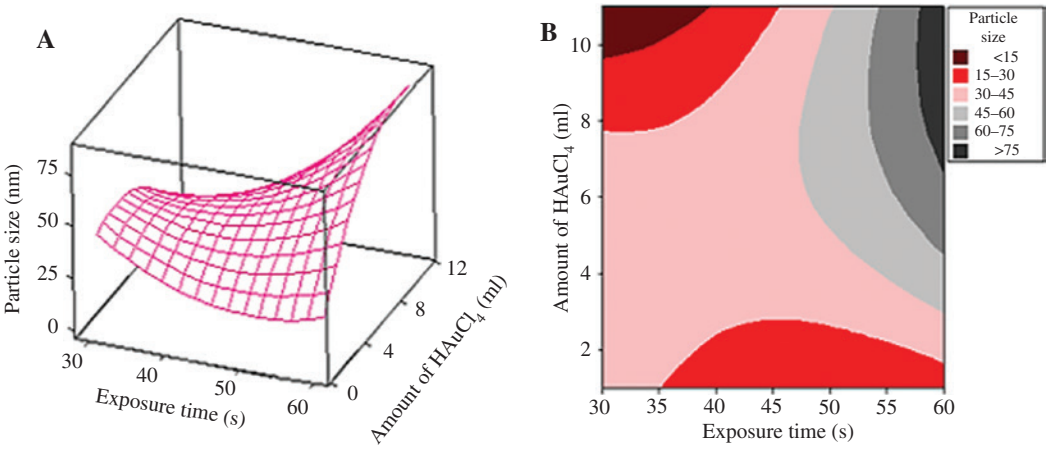

Figure 2: Response surface (A) and contour plots (B) for the mean particle size of produced AuNP solution as function of significant ($p < 0.05$) interaction effects of microwave exposure time and amount of $HAuCl_4$ solution.

the biosynthesis of AgNPs using aloe vera extract. They observed that the carbonyl group of proteins in aloe vera leaf extract adsorbed strongly to silver metals and reduced the agglomeration of the synthesized NPs.

3.4 Concentration of synthesized AuNPs

The concentration of the obtained AuNPs ranged from 83.09 to 152.45 ppm for different samples (Table 1). The changes in the concentration of AuNPs could also be explained as a function of microwave exposure time and the amount of HAuCl4 solution (Figure 3). The main effect of microwave exposure time was retained in the model because of its significant interaction effect ($p < 0.05$) with $HAuCl_4$ (Table 3). As clearly observed in Table 3, the microwave exposure time affected the AuNP concentration of systems more significantly as compared with the amount of $HAuCl_4$. Therefore, microwave exposure time showed to be the most vital parameter in the determination of this response. As clearly observed in Figure 3A, at low amounts of $HAuCl_4$ solution, by increasing the microwave exposure time, the concentration of the formed AuNPs increased and then decreased. However, at high amounts of $HAuCl_4$, the concentration of the synthesized AuNPs was increased by increasing the microwave exposure time. In fact, the minimum concentration of the synthesized AuNPs was obtained at minimum microwave exposure time and maximum amount of $HAuCl_4$ solution. Maximum AuNP concentration was formed at the central range of microwave exposure time and minimum amount of $HAuCl_4$ solution (Figure 3B). The obtained result can be explained by the fact that at low amounts of $HAuCl_4$ by the addition of constant mushroom extract, all the free gold ions were rapidly reduced to AuNPs. After that, by increasing the microwave radiation time, the temperature of the colloidal solution increased, which in turn enhanced the moving speed of the formed AuNPs and the collision frequency between NPs [14, 31].

3.5 Optimization of synthesis parameters for the AuNPs production

The AuNP synthesis would be optimized when the process resulted to the synthesized AuNPs with the smallest PDI and mean particle size and the highest concentration. For this reason, graphical optimization based on an overlaid contour plot was used to find the optimum region for the synthesis parameters (Figure 4). The indicated white colored area in Figure 4 demonstrated the desired microwave exposure time and the amount of $HAuCl_4$ solution to get the optimum AuNPs. A numerical multiple optimization was also used to find the exact optimum values of studied synthesis variables. The results also demonstrated that the synthesis conditions with a 2.62-ml $HAuCl_4$ and a 55-s microwave exposure time for the preparation of AuNPs would give the most desirable NPs. At the optimum conditions, AuNPs were fabricated with a mean particle size of 35.32 nm, a PDI of 0.876, and a concentration of 146.10 ppm. Moreover, three AuNP solutions were synthesized based on the suggested optimal values by numerical multiple optimization and characterized in terms of studied response variables. The measured experimental values for the mean particle size, PDI, and concentration of the synthesized AuNPs were 33.56 ± 1.8 nm, 0.855 ± 0.02

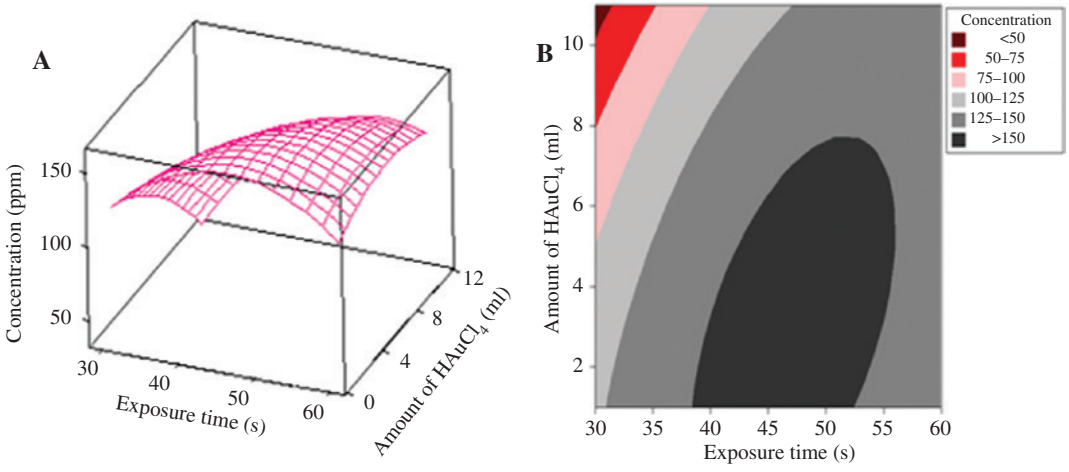

Figure 3: Response surface (A) and contour plots (B) for AuNP concentration of produced NPs solution as function of significant ($p < 0.05$) interaction effects of microwave exposure time and amount of $HAuCl_4$ solution.

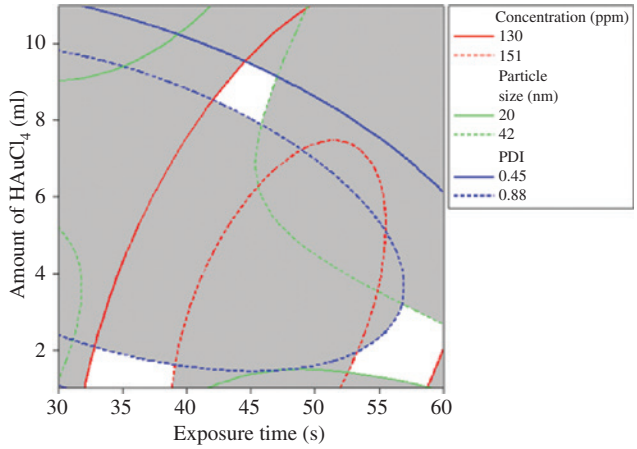

Figure 4: Overlaid contour plot of AuNPs particle size, concentration, PDI with acceptable levels as function of microwave exposure time, and amount of $HAuCl_4$ solution.

ppm, and 148.88 ± 2.7 ppm, respectively. The insignificant differences found between the predicted and the experimental values of the optimum suggested a sample that was reconfirmed by the adequacy of the fitted models for studied responses.

3.6 Physicochemical characteristics of synthesized AgNPs at obtained optimum conditions

3.6.1 Color of AuNP solution

By synthesis of the AuNPs at the optimum conditions, the color of the reaction mixture was turned into ruby red. The color change of the mixture, containing mushroom extract, $HAuCl_4$ solution, and synthesized AuNPs, is schematically shown in Figure 5. The color change occurred because of the presence of the active molecules in the mushroom extract, which could reduce the gold metal ions into AuNPs. The formation of AuNPs from the 1-mM solution of $HAuCl_4$ was confirmed by using UV-Vis spectral analysis (Figure 6).

UV-Vis spectroscopy involves the absorption of light by molecules in the UV-Vis region and can be used to determine the color changes and concentration of the formed NPs solution based on the absorbance [18]. Generally, AuNPs absorb in the visible region of the electromagnetic spectrum at 510–570 nm because of SPR transition [32]. Metal NPs have free electrons, which cause an SPR absorption band because of their combined vibration in resonance with the light wave [1, 33]. An SPR spectrum for AuNPs was obtained at 552 nm, as shown in Figure 7.

3.6.2 Particle size and zeta potential of synthesized AuNPs

The size distributions of these samples were also shown in Figure 8. The size distribution of the produced AuNPs was

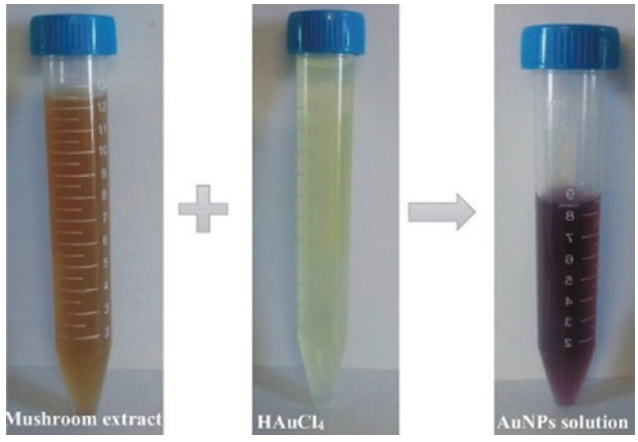

Figure 5: Schematic of color change in AuNP synthesis using mushroom extract.

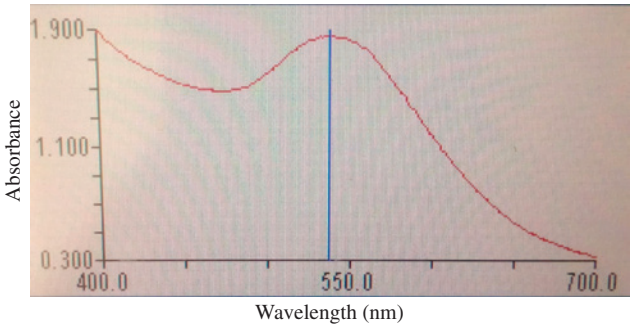

Figure 6: UV-Vis spectra of the mixture solution containing $HAuCl_4$ and mushroom extract, after synthesis with exposure to microwave irradiation at obtained optimum synthesis conditions.

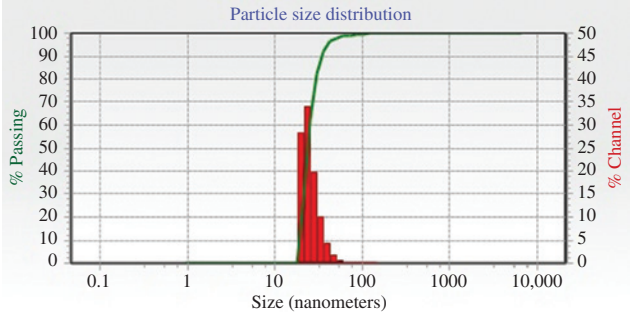

Figure 7: Dynamic light scattering (DLS) of the synthesized AuNPs.

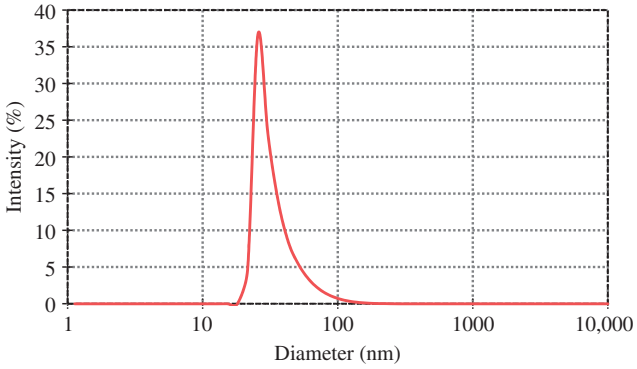

Figure 8: Size distribution of synthesized AuNPs at obtained optimum synthesis conditions.

monomodal (Figure 8). The monomodal size distribution was favored as compared with polymodal distribution because the polymodal particle distribution can speed up the Oswald ripening of particles and decrease the physical stability of NPs systems [23]. Therefore, the obtained monomodal NPs systems would have better long-term stability than the polymodal ones.

3.6.3 Morphology of synthesized AuNPs

TEM analysis was conducted to evaluate the shape and microstructure of the synthesized AuNPs. A typical TEM image of the synthesized AuNPs is shown in Figure 9. As clearly observed, the synthesized NPs were well dispersed with spherical structures. In fact, spherical NPs were more abundant than NPs of other shapes. This spherical shape indicated that the synthesized NPs had minimum surface energy and high thermodynamic stability, which confirmed the high value of the zeta potential of the synthesized AuNPs. The obtained results were in agreement with the finding of Bhat et al. [21]. They indicated that the edible mushroom *P. florida* extract could be used to biosynthesize spherical AuNPs with the particle size ranging from 10 to 50 nm. Philip [20] used the edible mushroom *V. volvacea* for AuNP synthesis, and the TEM images showed a successful synthesis of triangular nanoprisms to nearly spherical and hexagonal with different sizes between 20 and 150 nm. Das et al. [15] used *Calotropis procera* latex by microwave method for AuNP synthesis. They found that the particle size of AuNPs was 13 ± 5 nm and the shape of them was spherical. Rastogi and Arunachalam [16] used aqueous garlic (*Allium sativum*) extract in AuNP synthesis using microwave irradiation. The produced NPs were 23.2 nm in size and were mostly spherical in shape.

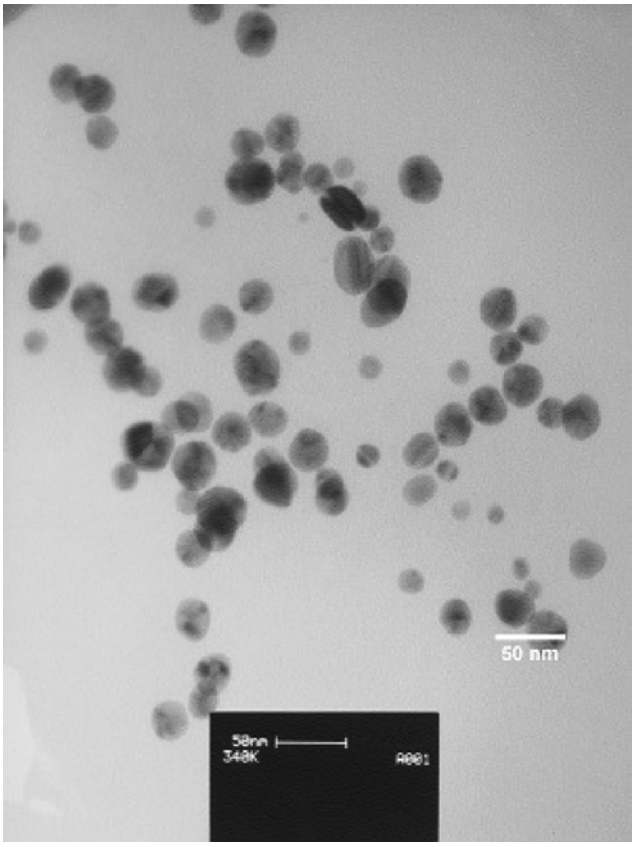

Figure 9: TEM image of the synthesized AuNPs using mushroom extract.

3.7 Antibacterial activity

The antibacterial activity of the synthesized AuNPs was evaluated by bacterial growth inhibition (lack of turbidity) in the 96-well plate. Table 4 shows the turbidity of the 96-well plate before and after a 24-h incubation at 37°C for both Gram-negative and Gram-positive bacteria. As clearly observed, there were insignificant differences between turbidity values of the wells containing AuNPs and *E. coli* and AuNPs and *S. aureus*. However, the mushroom extract did not show antibacterial activity toward both Gram-negative and Gram-positive bacteria, and the synthesized AuNPs showed high antibacterial activity toward them (Table 4). The obtained results can be explained by the fact that AuNPs have the potential to kill the cells by entering the bacterial cell wall. In fact, AuNPs could interact with the anionic groups of the cell wall components and structurally change the cell surface. A large number of AuNPs could strongly bond to the polycyclic aromatic hydrocarbon on the bacterial cell wall and create polyelectrolyte complexes, which could prevent the transport of essential solutes into the cell [31,

Table 4: Growth inhibition activity of the synthesized AuNPs against *S. aureus* (Gram-positive) and *E. coli* (Gram-negative).

	Negative control	Positive control	Mushroom extract	AuNPs
Gram positive (*S. aureus*)				
Before incubation	0.042	0.047	0.091	0.067
After incubation	0.047	0.306	0.307	0.075
Difference	0.005	0.259	0.216	0.008
Gram negative (*E. coli*)				
Before incubation	0.014	0.013	0.092	0.034
After incubation	0.018	0.211	0.311	0.038
Difference	0.004	0.198	0.219	0.004

Data are presented as the mean value of three replicates.

34, 35]. The results also demonstrated that the mean difference of turbidity value for the wells containing AuNPs and *E. coli* was less than that of the wells, including AuNPs and *S. aureus*. Therefore, it seems that the antibacterial activity of the synthesized AuNPs was stronger on Gram-negative bacteria than Gram-positive bacteria. Several studies have also shown that AuNPs were more effective on the Gram-negative bacteria as compared with the Gram-positive bacteria [36]. El-Sayed et al. [37] reported that the 20–50-nm AuNPs indicated the most efficient cellular uptake, and specific cell toxicity was related to the AuNPs with particle size of 40–50 nm. The small size of the synthesized AuNPs (33.56 ± 1.8 nm) from the present study can effectively increase their antibacterial activity [37].

4 Conclusion

A rapid one-step green approach based on microwave irradiation was developed for AuNP synthesis without using any toxic chemicals. Edible mushroom (*A. bisporus*) extract acted mainly as both reducing and stabilizing agents during AuNP synthesis. The results indicated the usefulness of RSM for studying the effects of the synthesis conditions on the dependent variables and to optimize them to get the most desirable AuNPs. The fabricated AuNPs showed significant antibacterial activity against *E. coli* and *S. aureus*. This rapid synthesis method developed from the present study can be used as a favorable technique for the synthesis of other noble metal NPs.

Acknowledgments: The authors acknowledge the Iran Nanotechnology Initiatives Council (INIC) for funding (grant no. 84465) the development of innovative methodology for safety assessment of industrial nanomaterials.

References

[1] Huang X, El-Sayed MA. Gold nanoparticles: optical properties and implementations in cancer diagnosis and photothermal therapy. *J. Adv. Res.* 2010, 1, 13–28.
[2] Wen L, Lin Z, Gu P, Zhou J, Yao B, Chen G, Fu J. Extracellular biosynthesis of monodispersed gold nanoparticles by a SAM capping route. *J. Nanopart. Res.* 2009, 11, 279–288.
[3] Badwaik VD, Vangala LM, Pender DS, Willis CB, Aguilar ZP, Gonzalez MS, Paripelly R, Dakshinamurthy R. Size-dependent antimicrobial properties of sugar-encapsulated gold nanoparticles synthesized by a green method. *Nanoscale Res. Lett.* 2012, 7, 1–11.
[4] Singh AK, Talat M, Singh D, Srivastava O. Biosynthesis of gold and silver nanoparticles by natural precursor clove and their functionalization with amine group. *J. Nanopart. Res.* 2010, 12, 1667–1675.
[5] El-Batal AI, Hashem A-A, Abdelbaky NM. Gamma radiation mediated green synthesis of gold nanoparticles using fermented soybean-garlic aqueous extract and their antimicrobial activity. *SpringerPlus* 2013, 2, 129–139.
[6] Shamim N, Sharma VK, eds., *Sustainable Nanotechnology and the Environment: Advances and Achievements, ACS Symposium Series*. American Chemical Society: Washington, DC, 2013.
[7] Shang Y, Min C, Hu J, Wang T, Liu H, Hu Y. Synthesis of gold nanoparticles by reduction of HAuCl 4 under UV irradiation. *Solid State Sci.* 2013, 15, 17–23.
[8] Abbasi AR, Kalantary H, Yousefi M, Ramazani A, Morsali A. Synthesis and characterization of Ag nanoparticles@ polyethylene fibers under ultrasound irradiation. *Ultrason. Sonochem*. 2012, 19, 853–857.
[9] Ashassi-Sorkhabi H, Rezaei-moghadam B, Bagheri R, Abdoli L, Asghari E. Synthesis of Au nanoparticles by thermal, sonochemical and electrochemical methods: optimization and characterization. *Phys. Chem. Res*. 2015, 3, 24–34.
[10] Pal A, Shah S, Devi S. Microwave-assisted synthesis of silver nanoparticles using ethanol as a reducing agent. *Mater. Chem. Phys*. 2009, 114, 530–532.
[11] Horikoshi S, Serpone N, eds. *Microwaves in Nanoparticle Synthesis: Fundamentals and Applications*. John Wiley & Sons: New York, 2013.
[12] Patel K, Kapoor S, Dave DP, Mukherjee T. Synthesis of nanosized silver colloids by microwave dielectric heating. *J. Chem. Sci*. 2005, 117, 53–60.

[13] Shirke B, Patil A, Hankare P, Garadkar K. Synthesis of cerium oxide nanoparticles by microwave technique using propylene glycol as a stabilizing agent. *J. Mater. Sci. Mater. Electron.* 2011, 22, 200–203.
[14] Vázquez A, Aguilar-Garib J, López I, Cavazos O, Gómez I. Preparation of ZnS nanoparticles using microwave assisted synthesis: effects of the irradiation power and the precursors. *Rev. Mex. Fís.* 2009, 55, 57–60.
[15] Das RK, Babu PJ, Gogoi N, Sharma P, Bora U. Microwave-mediated rapid synthesis of gold nanoparticles using *Calotropis procera* latex and study of optical properties. *ISRN Nanomater.* 2012, 2012, 1–6.
[16] Rastogi L, Arunachalam J. Microwave-assisted green synthesis of small gold nanoparticles using aqueous garlic (*Allium sativum*) extract: their application as antibiotic carriers. *Int. J. Green Nanotechnol.* 2012, 4, 163–173.
[17] Kasthuri J, Kathiravan K, Rajendiran N. Phyllanthin-assisted biosynthesis of silver and gold nanoparticles: a novel biological approach. *J. Nanopart. Res.* 2009, 11, 1075–1085.
[18] Mohammadlou M, Maghsoudi H, Jafarizadeh-Malmiri H. A review on green silver nanoparticles based on plants: synthesis, potential applications and eco-friendly approach. *Int. Food Res. J.* 2016, 23, 446–463.
[19] Palacios I, Lozano M, Moro C, D'arrigo M, Rostagno M, Martínez J, García-Lafuente A, Guillamón E, Villares A. Antioxidant properties of phenolic compounds occurring in edible mushrooms. *Food Chem.* 2011, 128, 674–678.
[20] Philip D. Biosynthesis of Au, Ag and Au-Ag nanoparticles using edible mushroom extract. *Spectrochim. Acta Mol. Biomol. Spectrosc.* 2009, 73, 374–381.
[21] Bhat R, Sharanabasava V, Deshpande R, Shetti U, Sanjeev G, Venkataraman A. Photo-bio-synthesis of irregular shaped functionalized gold nanoparticles using edible mushroom *Pleurotus florida* and its anticancer evaluation. *J. Photochem. Photobiol. B* 2013, 125, 63–69.
[22] Wilberley S, Sprague JW, Campbell J. Quantitative infrared analysis of solids in potassium bromide using an internal standard. *Anal. Chem.* 1957, 29, 210–213.
[23] Anarjan N, Jafarizadeh-Malmiri H, Nehdi IA, Sbihi HM, Al-Resayes SI, Tan CP. Effects of homogenization process parameters on physicochemical properties of astaxanthin nanodispersions prepared using a solvent-diffusion technique. *Int. J. Nanomed.* 2015, 10, 1109–1118.
[24] Shameli K, Ahmad MB, Jazayeri SD, Shabanzadeh P, Sangpour P, Jahangirian H, Gharayebi, Y. Investigation of antibacterial properties silver nanoparticles prepared via green method. *Chem. Cent. J.* 2012, 6, 73–83.
[25] Anarjan N, Jaberi N, Yeganeh-Zare S, Banafshehchin E, Rahimirad A, Jafarizadeh-Malmiri H. Optimization of mixing parameters for α-tocopherol nanodispersions prepared using solvent displacement method. *J. Am. Oil Chem. Soc.* 2014, 91, 1397–1405.
[26] Bezerra MA, Santelli RE, Oliveira EP, Villar LS, Escaleira LA. Response surface methodology (RSM) as a tool for optimization in analytical chemistry. *Talanta* 2008, 76, 965–977.
[27] Gharibzahedi SMT, Mousavi SM, Hamedi M, Khodaiyan F, Razavi SH. Development of an optimal formulation for oxidative stability of walnut-beverage emulsions based on gum arabic and xanthan gum using response surface methodology. *Carbohyd. Polym.* 2012, 87, 1611–1619.
[28] Narasimha G, Praveen B, Mallikarjuna K, Deva Prasad Raju B. Mushrooms (*Agaricus bisporus*) mediated biosynthesis of sliver nanoparticles, characterization and their antimicrobial activity. *Int. J. Nano Dimens.* 2011, 2, 29–36.
[29] Zhang Y, Cheng X, Zhang Y, Xue X, Fu Y. Biosynthesis of silver nanoparticles at room temperature using aqueous aloe leaf extract and antibacterial properties. *Colloids Surf. A. Physicochem. Eng. Asp.* 2013, 423, 63–68.
[30] Medda S, Hajra A, Dey U, Bose P, Mondal NK. Biosynthesis of silver nanoparticles from aloe vera leaf extract and antifungal activity against *Rhizopus sp.* and *Aspergillus sp. Appl. Nanosci.* 2015, 5, 875–880.
[31] Palza H. Antimicrobial polymers with metal nanoparticles. *Int. J. Mol. Sci.* 2015, 16, 2099–2116.
[32] Jafarizad A, Safaee K, Gharibian S, Omidi Y, Ekinci D. Biosynthesis and in-vitro study of gold nanoparticles using mentha and *pelargonium* extracts. *Procedia Mater. Sci.* 2015, 11, 224–230.
[33] Han JW, Gurunathan S, Jeong JK, Choi YJ, Kwon DN, Park JK, Kim JH. Oxidative stress mediated cytotoxicity of biologically synthesized silver nanoparticles in human lung epithelial adenocarcinoma cell line. *Nanoscale Res. Lett.* 2014, 9, 459–473.
[34] Kon K, Rai M. Metallic nanoparticles: mechanism of antibacterial action and influencing factors. *J. Comp. Clin. Pathol. Res.* 2013, 2, 160–174.
[35] Zhou Y, Kong Y, Kundu S, Cirillo JD, Liang H. Antibacterial activities of gold and silver nanoparticles against *Escherichia coli* and bacillus Calmette-Guérin. *J. Nanobiotechnol.* 2012, 10, 19–28.
[36] Saranya S. Biosynthesis of gold nanoparticles (AuNPs) from *C. orchioides* and study their antimicrobial efficacy. *Int. J. Phytopharm.* 2015, 5, 58–64.
[37] El-Sayed IH, Huang X, El-Sayed MA. Selective laser photo-thermal therapy of epithelial carcinoma using anti-EGFR antibody conjugated gold nanoparticles. *Cancer Lett.* 2006, 239, 129–135.

Bionotes

Maryam Eskandari-Nojehdehi
Faculty of Chemical Engineering, Sahand University of Technology, Tabriz 1996-51335, Iran

Maryam Eskandari-Nojehdehi was born and raised in the capital of Iran, Tehran. She obtained her BSc degree in food engineering in 2012. For her bachelor's degree thesis, she worked on the applications of carboxymethyl cellulose in food products. She obtained her MSc degree in chemical engineering with major on food engineering at Sahand University of Technology, Iran, in 2015. The present study is the results of her master's thesis under the supervision of Assistant Professor Hoda Jafarizadeh-Malmiri and Javad Rahbar-Shahrouzi. Her field of interest is the green synthesis of metal nanoparticles and the evaluation of their antimicrobial activity.

Hoda Jafarizadeh-Malmiri
Faculty of Chemical Engineering, Sahand University of Technology, Tabriz 1996-51335, Iran,
h_jafarizadeh@sut.ac.ir;
h_jafarizadeh@yahoo.com

Hoda Jafarizadeh-Malmiri was born in Yazd, Iran. He received his BSc and MSc degrees in food engineering (Iran). He obtained his PhD in food science at the Universiti Putra Malaysia in 2012. His PhD thesis was the extension of the shelf life of bananas using edible coating conjugated with silver nanoparticles. He joined Sahannd University of Technology, Iran, in 2012 and is currently working as an assistant professor at the Faculty of Chemical Engineering. He is the head of the Food Research Institute. His fields of interests include nanobiotechnology, food biotechnology, green processes, and organic and inorganic nanoparticle synthesis.

Javad Rahbar-Shahrouzi
Faculty of Chemical Engineering, Sahand University of Technology, Tabriz 1996-51335, Iran

Javad Rahbar-Shahrouzi was born in Tabriz, Iran. He received his BSc and MSc degrees in chemical engineering at the Petroleum University of Technology (2001) and Sharif University of Technology (2004), respectively. He obtained his PhD degree at the University of Paris six in process engineering (2010). He is now working as an academic staff in Sahand University of Technology since 2011. He is currently the vice dean of the Chemical Engineering Faculty. His areas of interest are nanosensor development and modeling, simulation, and process optimization.